Response of a stiff monopile for a long-term cyclic loading

Lada, Aleksandra; Gres, Szymon; Nicolai, Giulio; Ibsen, Lars Bo

Publication date:
2014

Document Version
Publisher's PDF, also known as Version of record

Response of a stiff monopile for a long-term cyclic loading

Aleksandra Lada
Szymon Gres
Giulio Nicolai
Lars Bo Ibsen

ISSN 1901-7278
DCE Technical Memorandum No. 45

DEPARTMENT OF CIVIL ENGINEERING
AALBORG UNIVERSITY

Aalborg University
Department of Civil Engineering

DCE Technical Memorandum No. 45

Response of a stiff monopile for a long-term cyclic loading

by

Aleksandra Lada
Szymon Gres
Giulio Nicolai
Lars Bo Ibsen

June 2014

Scientific Publications at the Department of Civil Engineering

Technical Reports are published for timely dissemination of research results and scientific work carried out at the Department of Civil Engineering (DCE) at Aalborg University. This medium allows publication of more detailed explanations and results than typically allowed in scientific journals.

Technical Memoranda are produced to enable the preliminary dissemination of scientific work by the personnel of the DCE where such release is deemed to be appropriate. Documents of this kind may be incomplete or temporary versions of papers—or part of continuing work. This should be kept in mind when references are given to publications of this kind.

Contract Reports are produced to report scientific work carried out under contract. Publications of this kind contain confidential matter and are reserved for the sponsors and the DCE. Therefore, Contract Reports are generally not available for public circulation.

Lecture Notes contain material produced by the lecturers at the DCE for educational purposes. This may be scientific notes, lecture books, example problems or manuals for laboratory work, or computer programs developed at the DCE.

Theses are monograms or collections of papers published to report the scientific work carried out at the DCE to obtain a degree as either PhD or Doctor of Technology. The thesis is publicly available after the defence of the degree.

Latest News is published to enable rapid communication of information about scientific work carried out at the DCE. This includes the status of research projects, developments in the laboratories, information about collaborative work and recent research results.

Published 2014 by
Aalborg University
Department of Civil Engineering
Sohngaardsholmsvej 57,
DK-9000 Aalborg, Denmark

Printed in Aalborg at Aalborg University

ISSN 1901-7278
DCE Technical Memorandum No. 45

Response of a stiff monopile for a long-term cyclic loading

Aleksandra Lada Szymon Gres Giulio Nicolai Lars Bo Ibsen
Aalborg University
Department of Civil Engineering

Abstract

In the Geotechnical Laboratory at Aalborg University a number of small scale tests have been performed to analyze the behavior of a rigid monopile subjected to a long-term cyclic lateral loading. Only a dense state of sand is considered. A cyclic loads cause the permanent displacement of soil and rotation of a pile, effecting in the accumulated rotation and the change in soil-pile stiffness. These aspects, as poorly accounted in current standards, require thorough analysis. The design methods and a current state of art in cyclic loading field is discussed. One of the aims of the article is to validate the method established by LeBlanc (2010) in order to confirm its reliability. In addition, the results of performed tests are presented to obtain the further conclusion on the cyclic behavior of monopiles.

1 Introduction

In the past few years a strong impact has been put on the contribution of the renewable energy sources in the total energy consumption. According to the statistics, the wind power is the leading renewable energy resource in Northern Europe. In Denmark, the data shows that wind energy contributes 27% to total electricity consumption and by 2025 it should rise to 50% [EWEA, 2013]. Among the wind energy structures the offshore wind turbines, OWT, withstand the most harsh and various environmental conditions, therefore a strong influence should be put on their design and the cost optimalization.

The foundation concept for OWT structures is very dependent on the site parameters. There are several types of foundations used: gravity based foundation, monopile foundation, jacket, tripod foundation and bucket foundation. For the average water depth, 10-30 m, the most common type of a foundation is a steel monopile. It consists of a large diameter steel tube driven directly into the seabed and connected with a tower through a transition piece. Currently used monopiles have diameters in range 4-7 m and slenderness ratio around 5. Average length of a monopile foundation is 15-40 m.

The monopile foundation concept for offshore wind turbines originates from the offshore oil and gas sector. However, the physical behavior and the loading type differ. An offshore wind turbine structure is exposed to a strong long-term cyclic lateral loading through it's lifetime due to environmental loads. The number of loading cycles that a structure must withstand varies depending on the situation. Storms cause approximately 1000 - 5000 cycles, where the FLS is assessed for 10^7 cycles.

As a consequence, it leads to rotation of a monopile and rearrangement of soil particles, causing changes in the natural frequency of a soil-structure system. As a result, it strongly influences the design criteria of all parts of a wind turbine. Hence the main design factor for OWT is serviceability limit state and a long-term cyclic lateral loading contributes to permanent deformations in soil and changes in the soil stiffness, therefore it is essential to predict the effects of horizontal loading on monopile foundation.
The 1g tests have being performed in the Geotechnical Laboratory at Aalborg University. A high-quality experimental equipment allows to perform static and both one-way and two-way cyclic tests for the pile under different long-term horizontal loading, with accurate displacements measurements.

In the article the results of tests performed by LeBlanc et al. [2010] are compared with the new test results in order to confirm the reliability of used methods. Another aim of the article is to draw further conclusion regarding the behavior of cyclic loaded monopiles.
The current research was started by M.G. Onofrei et al. [2012] and their results, among others, are used in further analysis.

2 Current design standards

Current design standards for monopile foundations embedded in sand are based on the empirically derived p-y curves approach,[API, 2005] and [DNV, 2011]. The approach was originally presented by Reese et al.[1974] and subsequently improved and re-formulated by Murchison and O'Neil [1984] by the full scale tests carried out on the Mustang Islands. Physically, p-y curves implemented to Winkler approach are described as series of uncoupled springs, showing a non-linear relation between the lateral displacement of the pile and the soil resistance. A non-linear soil behavior corresponds to the subgrade reaction modulus function. The numerical solution to this problem is provided by solving the 4th order differential equation for a beam deflection.
Recent design regulations define hyperbolic formulation for constructing the non-linear p-y curves for monopiles in sand, dependent on the ultimate soil resistance and the soil stiffness.

$$p(y) = A \cdot p_u \cdot tanh\left(\frac{k \cdot z}{A \cdot p_u \cdot y}\right) \qquad (1)$$

where

A	The loading coefficient
k	The initial modulus of subgrade reaction
p_u	The ultimate soil resistance
z	The soil depth

For a cyclic lateral loading coefficient A is equal 0.9. This indicates that the ultimate soil resistance is reduced. The method was empirically derived from few full scale test of very slender, flexible piles ($L/D = 34.4$). Currently used monopiles for OWT have the slenderness ration around 5. According to Poulos & Hull [1989] a pile behaves as a rigid when the equation (2) is fulfilled, whereas the flexible pile behavior is expected for piles that satisfied the equation (3), [Sørensen *et al.*, 2012].

$$L < 1.48 \cdot \left(\frac{E_p I_p}{E_s}\right)^{0.25} \qquad (2)$$

$$L > 4.44 \cdot \left(\frac{E_p I_p}{E_s}\right)^{0.25} \qquad (3)$$

For offshore steel monopiles in dense sand these expressions are presented in Figure 2.1. A thickness of a monopile wall is expressed as a function of a pile diameter, $t = D/80$. The limit values of Young's modulus for the dense sand, E_s, are considered.

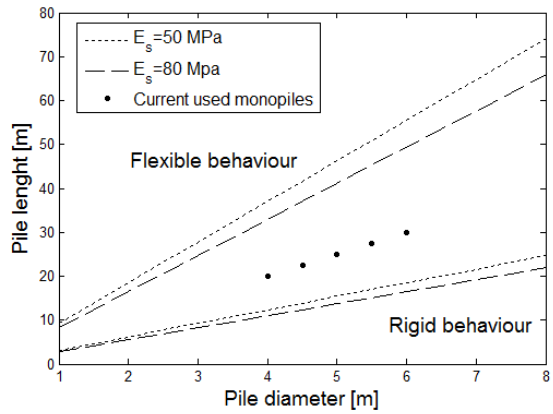

Figure 2.1: Criterion for a pile behavior

Even though, the currently used piles are not precisely fitted to rigid behavior, unquestionable they cannot be analyzed as flexible. Presently, the monopiles used offshore are considered as rigid. The difference in those two behavior of laterally loaded pile is presented in Figure 2.2. Due to different deformation pattern the soil-pile interaction changes, which could possibly influence the p-y curve formulation.

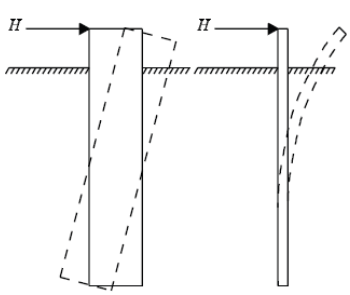

Figure 2.2: Difference between the rigid and the flexible pile behavior [Sørensen *et al.*, 2012]

In addition, OWT during its lifetime is subjected to a large number of cycles leading to accumulated rotation and hardening (or softening) of the soil. Moreover, the pile rotation and changes in soil stiffness are dependent on the direction and the magnitude of loading, which is presented hereafter. However, the p-y curve formulation neglects the influence of these loading parameters. Therefore current design standards are not reliable in describing the long term cyclic effects on a rigid monopile foundation. Methodology for cyclic loaded piles still requires further investigation.

3 State of art

Recently a number of research have been conducted in order to estimate the influence of a cyclic lateral loading on a monopile foundation. The number of proposed methods is vast, from full scale tests to the advanced numerical models and different kind of small-scale experiments. Some of the studies related to analyzed problem are presented.

Little & Briaud [1998] conducted research focuses on effects of a cyclic loading on piles lateral displacement. Obtained results are based on 6 full scale tests on slender piles with different material properties such as reinforced concrete, pre-stressed concrete and steel. These piles were subjected to $10 - 20$ number of cycles. The data was analyzed by using the cyclic p-y curve approach presented by Little & Briaud [1987], which describes a power law dependency between the number of cycles and the pile displacement.

$$y_N = y_1 \cdot N^{\alpha} \tag{4}$$

where

y_N	The lateral displacement after N cycles
y_1	The lateral displacement after 1st cycle
α	The cyclic degradation parameter

Results from research lead to the following conclusions:
- the traditional p-y curve approach overestimates a pile displacement during cyclic loading,
- a pile displacement obtained by the cyclic p-y curve approach are undervalued in compari-

son to the measured data,
- a pile-soil stiffness has a major influence on soil displacements,
- a soil densification occurs after the first series of cycles (around 10 cycles) resulting in a stiffer response during the second series.

Long & Vanneste [1994] analyzed results of 34 full scale tests conducted in the Tampa Bay, Florida, in order to investigate effects and parameters influencing a pile response to a repetitive lateral loading. Piles were subjected to varying number of cycles (50-100 cycles). The invented method includes the effects of loading characteristics, a pile installation method and a soil density. The equation (5), based on Little&Briaud solution, involves deterioration of a static p-y curve resistance to account all mentioned effects.

$$p_N = p_1 \cdot N^{(\alpha-1)t} \tag{5}$$

where

p_N	The soil resistance after N cycles
p_1	The soil resistance after 1st cycle
α	The degradation factor
t	The degradation parameter

A pile deflection obtained by using deteriorated static p-y curve method is more accurately fitted to full scale tests than deflection calculated by using the standard p-y curve approach.

Lin & Liao [1999] conducted a study in evaluating a strain accumulation for repetitive laterally loaded piles in sand. The data was obtained from 20 full scale tests performed for piles with varying slenderness ($L/D = 4.1 - 84.14$), number of cycles between $4 - 100$ cycles and different installation methods. The results confirmed that the cyclic strain ratio is determined by the load characteristics, the pile installation method, the soil properties and a relation between soil/pile stiffness. By definition of strain, cyclic strain ratio can be used to calculate pile head displacement ratio as following:

$$\frac{\varepsilon_N}{\varepsilon_1} = 1 + t \cdot ln(N) \tag{6}$$

where

ε_N	The soil strain after N cycles
ε_1	The soil strain after 1st cycle
t	The degradation parameter

The formula was additionally validated by 6 full scale tests. The predicted and measured displacements were in a good fit for the most of cycles, however during the last stage of loading there were some differences. It is assumed that it was caused by an increase of the soil density with the number of cycles.

LeBlanc *et al.* [2010] introduced an innovative approach based on 1g small-scale laboratory tests, where the predicted accumulated rotation and the change in stiffness of a pile-soil system were analyzed in relation to the load characteristics and the soil density. The tested pile was subjected to 8 000 - 60 000 number of cycles in realistic time frame. Different loading combinations were analyzed. Obtained results were scaled to the full scale through scaling law, allowing an accurate comparison to other results from full-scale tests.
The difference in the isotropic stress level between a small scale and a full scale test was included. A corresponding friction angle was achieved by lowering the relative soil density. The influence of the effective vertical stress was considered in shear modulus calculations. This experiment was conducted on a mechanical rig, where the cyclic loading characteristics were controlled by a system of pulleys and wires between the pile and weight hangers. Tests were performed with a use of the rigid cooper pile, ($L/D = 4.5$), embedded in dry sand. The research was performed for $I_D = 4\%$ and $I_D = 38\%$, corresponding to the loose and medium-dense state in full scale respectively. The deflections were measured by two dial gauges.

Figure 3.1: The mechanical rig used for tests

The analyzed data revealed an exponential correlation between the accumulated rotation and the number of cycles. Subsequently, the accumulated rotation was dependent on the magnitude and the loading direction. The obtained results showed that the maximum value for accumulated rotation is between one way and two way loading, which contradicts the general beliefs that the largest accumulated rotation is for one way cyclic loading. For the soil stiffness the logarithmic increase with the number of cycles was revealed. This change was observed as independent on the soil density, but only related to the load characteristics. This increase undermines the existing regulations used in standards, [DNV, 2011], indicating the degradation of p-y curves due to a cyclic loading.

4 Test Set-up

Based on the equipment used by LeBlanc et al. [2010], a similar rig has been constructed in the AAU laboratory. The research equipment is illustrated in Figure 3.1.

A cylindrical container is filled with sand of properties presented in Table 4.1. These parameters were obtained by previous tests performed in the laboratory. The inner diameter of the container is 2000 mm and the depth is equal to 1200 mm. At the bottom a drainage system is installed in order to provide saturation of sand. The system includes pipes and the gravel layer of 300 mm, covered by the geotextile.

Table 4.1: Properties of the sand used at Aalborg University Laboratory

Property	Value
Specific grain density, d_s [g/cm^3]	2.64
Maximum void ratio, e_{max} [-]	0.858
Minimum void ratio, e_{min} [-]	0.549

In order to simulate the offshore conditions, the sand must be fully saturated and dense. Before each test a hydraulic gradient is applied and a loose state of sand is obtained by reducing the effective stress. Next sand is vibrated mechanically in order to achieve a small void ratio. The density of soil is established through performing cone penetration tests, [Ibsen *et al.*, 2009]. The variation of the relative densities, I_D, from different tests is presented in Table 4.3. From the results it can be concluded that the soil conditions are similar between each performed test. The target results of I_D lay between 80 to 90 %, what indicates a dense state of sand.

Table 4.2: The variation of the relative soil density

Number of tests	μ_{I_D}	σ_{I_D}
15	88.34 %	4.12 %

An open-ended, aluminum pile is used for tests. The pile characteristics are presented in Table 4.3. The reason of chosen eccentricity is due to the expected eccentricity level of wave loads acting on a pile in the most common cases [Onofrei *et al.*, 2012]. The pile behavior is assumed to be rigid. The small variation of the load eccentricity, $\pm$ 5 mm, that can be caused by different level of soil, are included in the calculations of the moment on the seabed.

Table 4.3: Characteristics of the pile

Property	Length [mm]
Embedded length,L	500
Diameter,D	100
Slenderness ratio, $\frac{L}{D}$	5
Thickness, t	5
Load eccentricity, a	600 ± 5

The monopile is installed in sand by using an electrical motor working with the velocity of 0.02 mm/s. This ensures a small disturbance of the soil.

The different part of the rig are presented in Figure 4.1 and described hereafter.

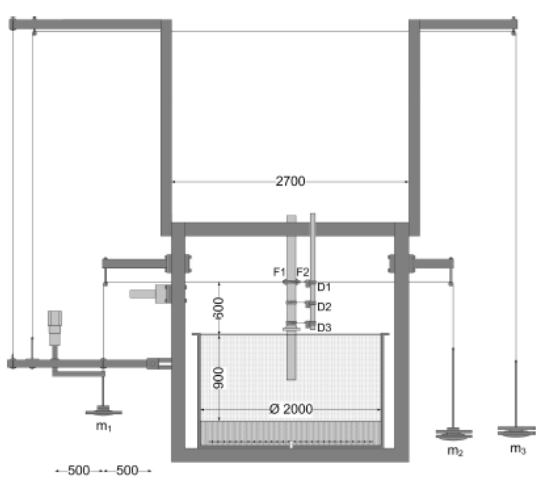

Figure 4.1: A test set-up with the dimensions and the localizations of transducers [Onofrei *et al.*, 2012]

At the top of the pile a rigid tower with force transducers is mounted, F_1 and F_2. A steel frame situated above the container consists of a system of pulleys and wires, that are used to transfer the loads from weights, m_1, m_2 and m_3, to the rigid tower. A beam with three displacement transducers, D_1, D_2 and D_3, is fixed to the steel frame in order to measure the displaced position of the pile. This information are used to extrapolate a rotation to the ground level. Two types of loading are performed, indicating the two different loading systems.
The static loading is a displacement controlled test performed with the use of a motor attached to the steel frame. The motor creates a pulling horizontal force acting on the tower, which is recorder by F_1. The main aim of this test is to obtain the ultimate resistance moment of soil, M_R. The speed of pulling is equal to 0.02 mm/s, so in case of creating the excess pore pressure, it can easily dissipate.
A cyclic loading is initiated by m_1 and m_2, which create forces recorded by F_1 and F_2. The mass m_3 is a counter-weight of the rig. The mass m_2 is directly connected to F_2 through a wire and a pulley, what result in the force equal to $m_2 g$. On the other side the mass m_1 is put on a rotating hanger, controlled by a motor with the loading frequency of 0.1 Hz. This correspond to a common wave loads frequency [Onofrei *et al.*, 2012].

The rotating hanger works on a lever connected to the frame through a pinned joint. When the motor starts to rotate m_1, the force increases until it reaches the maximum value, when the mass is in the most further position, equation (7). While the cycle is continued, the force decreases till minimum, when the mass returns to the starting position - the most closest to the force transducers, equation (8).

$$F_{max} = 3 \cdot m_1 g - m_2 g \tag{7}$$

$$F_{min} = m_1 g - m_2 g \tag{8}$$

An accurate determination of the loading magnitude is difficult due to the loss in force. Partly, it can be caused by the friction in the mechanical system. In addition, some losses appear due to the lever tilting. As long as the wire connecting F_1 and the lever is of a fixed length, every time when the pile rotates, the position of the lever will change in some small extent.

5 Tests methodology

A presented research methodology is based on the concept described by LeBlanc *et al.* [2010]. A comparison with the full-scale is not a part of the research, therefore no scaling law is used.

All tests are identified by the load characteristic parameters ζ_b, equation (9) and ζ_c, equation (10). The cyclic loading parameters describe the magnitude and direction of loading respectively. The visual interpretation is illustrated in Figure 5.1.

$$\zeta_b = \frac{M_{max}}{M_R} \tag{9}$$

$$\zeta_c = \frac{M_{min}}{M_{max}} \tag{10}$$

where

M_{max}	The maximum moment[Nm]
M_{min}	The minimum moment [Nm]
M_R	The static moment capacity [Nm]

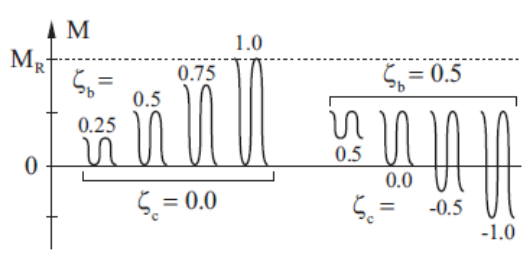

Figure 5.1: Characterization of cyclic loading [LeBlanc *et al.*, 2010]

The value of the static moment capacity is obtained from a static loading test. The value of M_R is determined in reference to moment-rotation curves. The moment of failure is identified for the maximum value, before the magnitude starts to decrease. The results of static tests are illustrated in Figure 5.2.

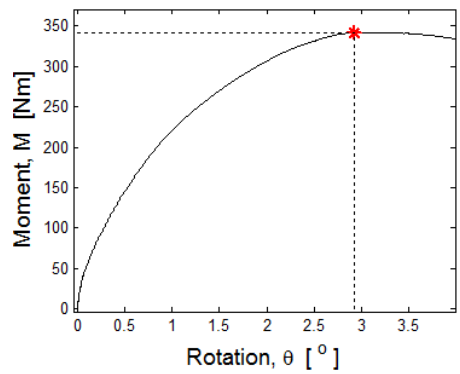

Figure 5.2: The static test results

The applied magnitude of loading is determined in reference to FLS, where ζ_b for the typical design load for OWT fluctuates around value of 0.3. The assumed range of ζ_c is $-1 < \zeta_c < 1$, where $\zeta_c = 1$ describes the one-way loading and $\zeta_c = -1$ describes the two-way loading. The research pays attention on the negative values of ζ_c, regarding to the conclusion made by LeBlanc *et al.* [2010], that the worse cyclic conditions are obtained for tests with loading between one-way and two-way.

The data obtained in tests provide information about the change in stiffness during the cyclic loading, k, and the accumulated rotation after long-term cyclic loading, $\Delta\theta(N)$. The assumptions concerning these two parameters are described in following sections. The method for determining both values is presented in Figure 5.3.
During the cyclic test 50 000 load cycles are applied. The FLS is assessed for 10^7 number of cycles, however such a big number of cycles

is time consuming. The adopted number of cycles is assumed to be sufficient for describing the behavior of monopiles for FLS.

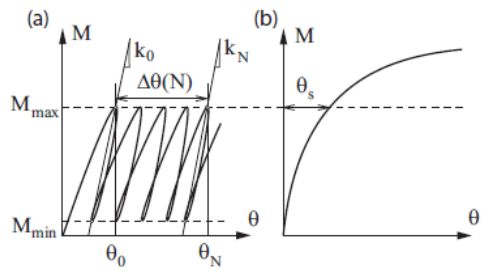

Figure 5.3: A method for determining stiffness and accumulated rotation [LeBlanc *et al.*, 2010]

In order to fully refer to the research performed by LeBlanc *et al.* [2010] the sand should behave as drained during the loading. As far as for static tests this is provided by the small velocity of pulling, the conditions during cyclic tests must be analyzed. Therefore, the results of first cycle in each test, the maximum moment and the corresponding rotation, are plotted and compared with the static results. Figure 5.4 indicates that during the cyclic tests, the drained condition is preserved. The only result that does not fit to the static curve is from the test characterized with $\zeta_b = 0.41$, where the sand behaviour can be interpreted as a partially drained.

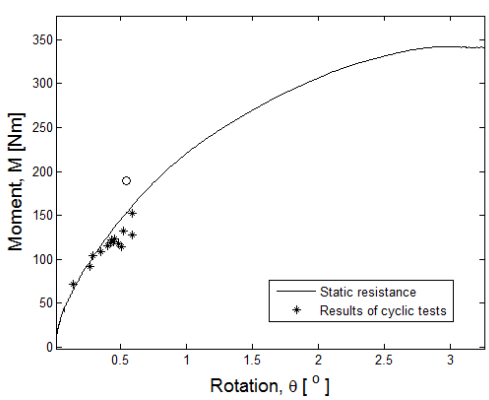

Figure 5.4: The reference static test with the results for first cycle in each cyclic test

6 The accumulated rotation

A method for describing accumulated rotation is express by equation (11), using the power law of the same form as it was done in LeBlanc *et al.* [2010].

$$\frac{\Delta\theta(N)}{\theta_0} = \frac{\theta_N - \theta_0}{\theta_0} = T_b \cdot T_c \cdot N^n \qquad (11)$$

where

θ_0	The rotation after 1st cycle
θ_N	The rotation after N cycle
T_b and T_c	Dimensionless functions
n	The power fitting parameter

It was already proved by others researchers, that the power dependency between the accumulated rotation and the number of cycles gives a good fit with the real tests values.
The magnitude of the rotation caused by cyclic loading should be normalized by the corresponding rotation from the static tests, θ_s, Figure 5.3. However, some differences between static moment capacity was revealed after performing few static tests in the AAU laboratory, as there are always some small discrepancies in the test set-up between performed tests. Furthermore, while the two-way cyclic tests are being performed, there is a risk of a small negative rotation to occur before the 1st cycle, what might have effects on the initial rotation. Therefore, the initial rotation is used when normalizing $\Delta\theta(N)$.

LeBlanc *et al.* [2010] revealed that a power fitting parameter for all loading conditions can be set to $n = 0.31$. However, this fit is not valid for dense sand, as illustrated in Figure 6.1 for one-way and two-way loading tests ($\zeta_c = -0.55$).
The fitting parameter is therefore adjusted for each singular test. So far, no dependency between power fitting parameters and load characteristics have been found, however the mean value for all tests is $n = 0.14$, which is a

half of the value given by LeBlanc.

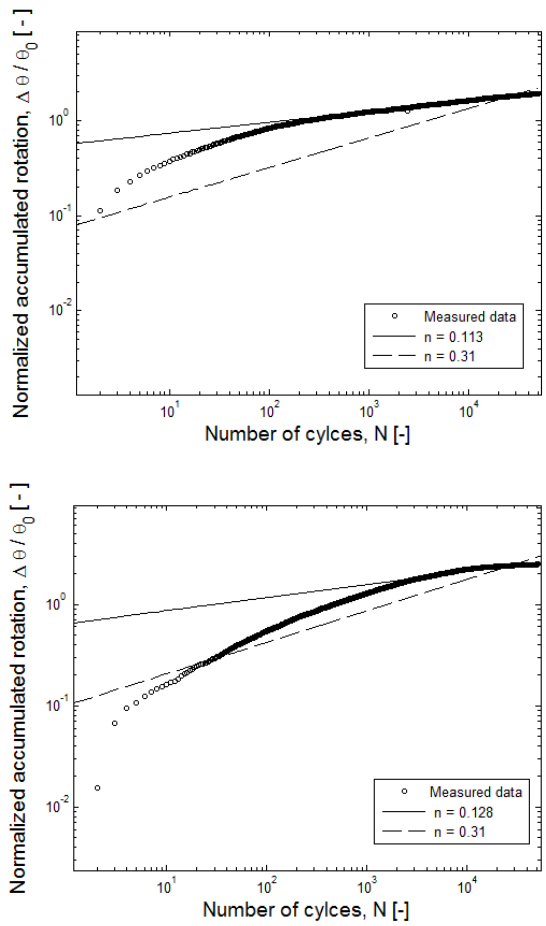

Figure 6.1: Normalized rotation for one-way loading test (upper plot) and two-way loading test (lower plot)

T_b and T_c functions depend on the load characteristics and soil density. T_b can be obtained by performing tests with $\zeta_c = 0$ and varying ζ_b. Figure 6.2 presents the relation of T_b for performed tests in correlation to the results obtained by LeBlanc *et al.* [2010]. The change in soil relative density seems to increase the values of T_b, what could indicate the increase of the accumulated rotation. However, as a different power fitting parameter is applied, the value of accumulated rotation cannot be solely based on T_b value.

It is assumed that $T_c(\zeta_c = 0) = 1$. As for the static test no accumulated rotation is expected, therefore $T_c(\zeta_c = 1) = 0$. The same is predicted for two-way cyclic loading, as the load is equal in both direction, $T_c(\zeta_c = -1) = 0$. The rest of the values are empirically determined by fitting to the laboratory results. Only the negative values of ζ_c are analyzed. Figure 6.3 illustrates the tests results, along with the trend found by LeBlanc *et al.* [2010].

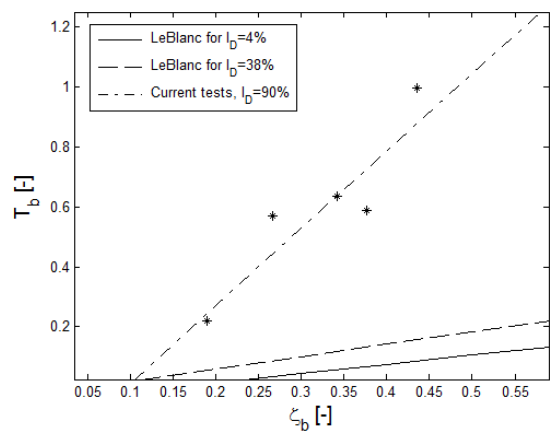

Figure 6.2: A dimensionless functions T_b

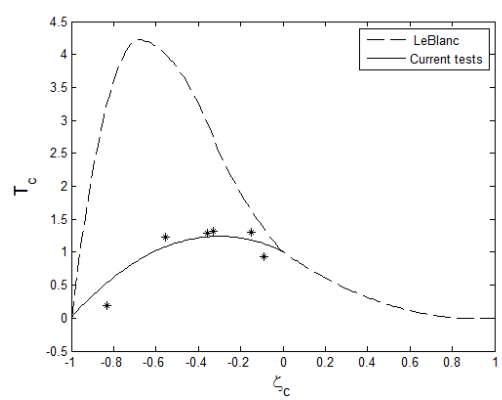

Figure 6.3: A dimensionless function T_c

Despite that the values of T_c are smaller in comparison with LeBlanc *et al.* [2010], it does not indicate that the accumulated rotation is smaller for denser sand, as it depend on both,

T_b and T_c. Both these values could be also affected by a power fitting parameter. However, the shapes of functions are similar, with extreme values for tests between one-way and two-way loading.

More results of accumulated rotation with dependency on ζ_c are presented in Figure 6.4 with logarithmic axes and in Figure 6.5 with normal axes. Selected tests are described by $\zeta_b \approx 0.3$.

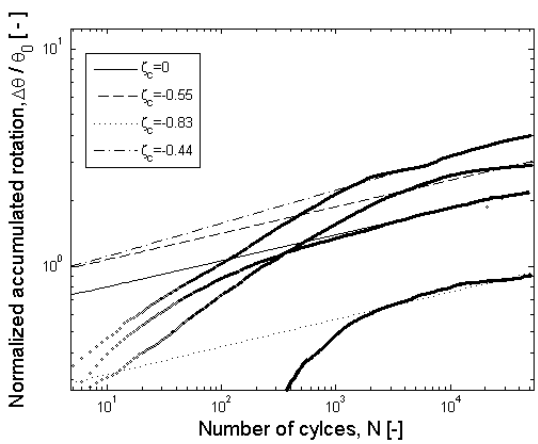

Figure 6.4: The increase of accumulated rotation for varying ζ_c - logarythmic axes

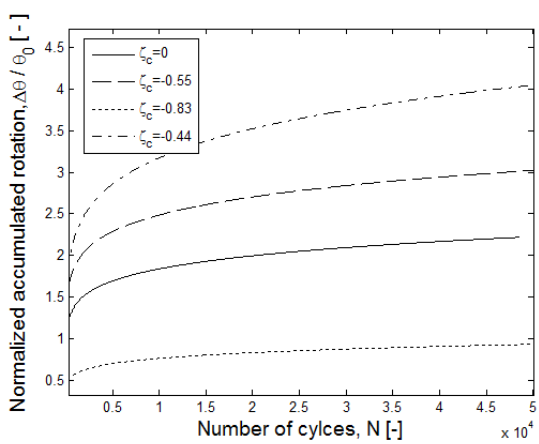

Figure 6.5: The fitting function for accumulated rotation for varying ζ_c - normal axes

The value of $\Delta\theta$ / θ_0 is overestimated by the power function for the first loading cycles, but a good fit is provided for a large number of cycles, what is crucial for FLS design. The accumulated rotation gets the biggest value for $\zeta_c = -0.44$, whereas the smallest increase is observed for $\zeta_c = -0.83$. Similar observation was obtain by LeBlanc *et al.* [2010], where the maximum accumulated rotation was obtained for loading condition between one-way and two-way. When the fitting functions are plotted in normal axes a significant accumulated rotation can be observed for couple first cycles and more constant behavior is found with increasing N.

Generally, the values of $\Delta\theta$ / θ_0 are bigger for dense sand in comparison to loose and medium-dense sand.

7 The change in stiffness

The stiffness in relation to the number of cycles, k_N, is described by the equation 12, likewise in the research of LeBlanc *et al.* [2010].

$$k_N = k_0 + A_k \cdot ln(N) \tag{12}$$

$$k_0 = K_b(\zeta_b)K_c(\zeta_c) \tag{13}$$

where

A_k	A dimensionless parameter
k_0	The initial stiffness
K_b and K_c	Dimensionless functions

Even though a larger scatter of data is noticeable for stiffness results, they can be fitted to above mentioned function. The dimensionless parameter A_k was found to be constant for results obtained by LeBlanc *et al.* [2010], $A_k = 8.02$, not depending on I_D.

Figure 7.1 presents the results for dense sand, where the data are fitted for fixed value of A_k in comparison to the best possible fit. The results reveal that for dense sand the parameter A_k is of larger value. The parameter is obtained for each test.

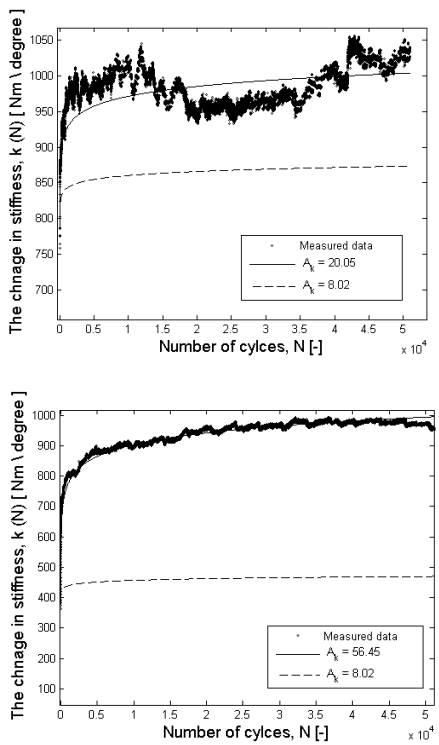

Figure 7.1: The change in stiffness for one-way loading test (upper plot) and two-way loading test (lower plot)

A large discrepancy of A_k is observed, but clearly there is an increase in A_k for increasing ζ_b, what can be found in Figure 7.2. No such a dependency was found for different values of ζ_c.

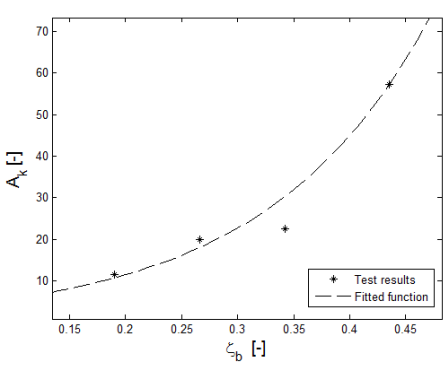

Figure 7.2: The increase of A_k as a function of ζ_b

According to LeBlanc *et al.* [2010] the dimensionless function K_b and K_c are only dependent on the load characteristics. In order to distinguish between two functions it is assumed that $K_c(\zeta_c = 0) = 1$, so the values of K_b are found for one-way cyclic loading and the rest of tests results are extrapolated. Functions are presented in Figure 7.3 and 7.4 along with the results obtained by LeBlanc *et al.* [2010].

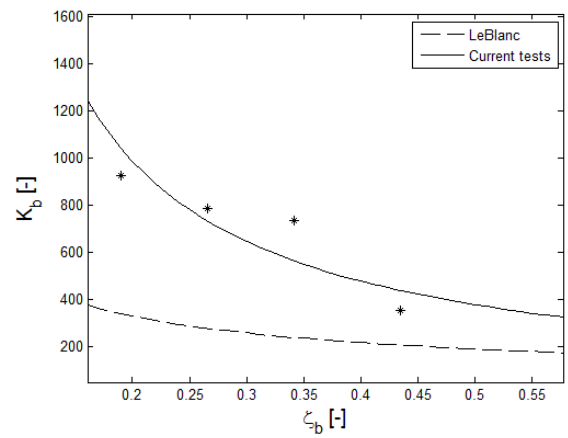

Figure 7.3: The dimensionless functions K_b

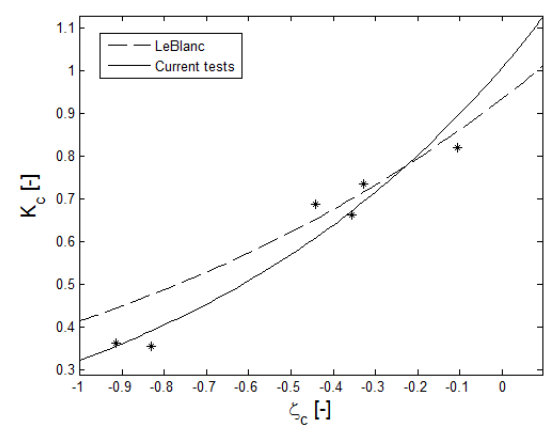

Figure 7.4: The dimensionless functions K_c

The results for dense sand indicate the increase in the initial stiffness comparing to loose and medium sand. The values of K_c, despite a visible scatter of data, seem to fit the curve ob-

tained by LeBlanc *et al.* [2010], whereas there is a significant increase in the values of K_b. The same trend is preserved, as an increase of ζ_b decreases the value of K_b. It can be concluded that values of K_c are independent on I_D, however this does not hold for values of K_b.

More results of the change in stiffness for changing ζ_c are presented in Figure 7.5. Selected tests are described with $\zeta_b \approx 0.3$.
The biggest increase of stiffness is observed for one-way cyclic loading, whereas the smallest increase occurred for the two-way loading test. The same behaviour was obtain by LeBlanc *et al.* [2010]. Furthermore, the most of soil stiffness is mobilized during first loading cycles. This behavior indicates a high, nonlinear increase is soil stiffness, that occurs due to cyclic sequence of loading and unloading, which might influence the relative soil density around the pile by increasing it. With increasing N, the value becomes more constant.

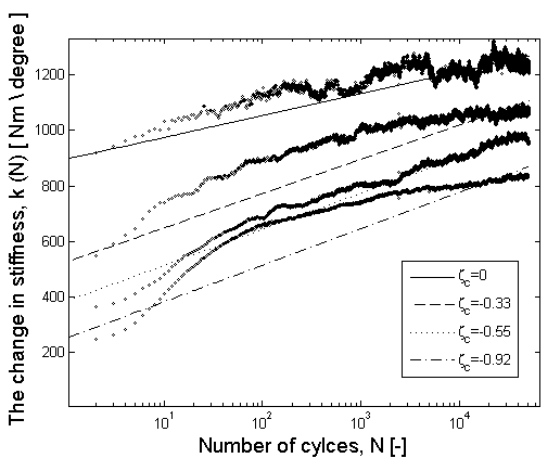

Figure 7.5: The change of stiffness for varying ζ_c

Generally, the increase of stiffness is found to be much bigger for dense sand in comparison to loose and medium-dense sand.

8 The post-cyclic soil resistance

The results reveals that the ultimate resistance almost always increases as a result of large number of cycles, Figure 8.1. The increase might be caused by the previously mentioned rise in the soil stiffness in the cyclic loading. The significant increase of the static stiffness is also noticed from the figure.

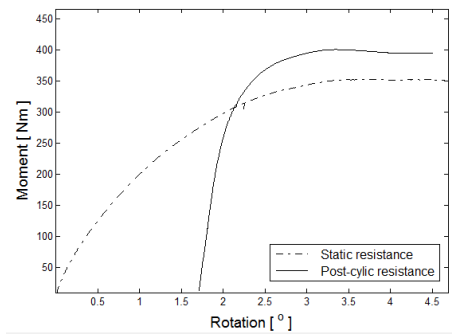

Figure 8.1: The change in soil ultimate resistance for one-way loading test

The results of post-cyclic resistance for all tests are plotted in Figure 8.2. All of the points exceed the ultimate bearing capacity given by the static tests. The average increase of the bearing capacity is assessed for around 10%.

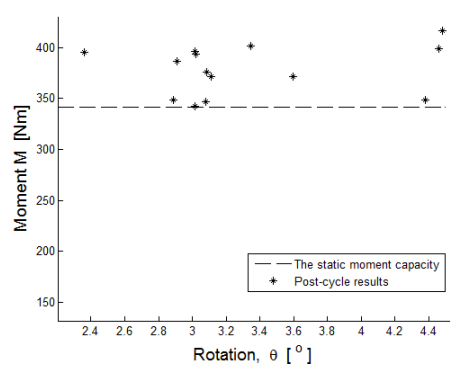

Figure 8.2: The results of the post-cyclic resistance for different tests

9 Conclusions

The presented paper provides the results of small scale tests conducted on the rigid pile foundation in dense, saturated sand. The monopile is subjected to a long-term cyclic lateral loading. The article relates to the results obtained by LeBlanc *et al.* [2010] for laterally loaded pile in loose and medium dense sands.

In the research the accumulated rotation and the change in cyclic stiffness are analyzed. Both illustrate that the loading characteristics have a significant effects on the pile behavior under a cyclic loading conditions. This finding is an important aspect for a future pile design, as the current standards do not include the load characteristics while designing a monopile subjected to the cyclic loading.
The function for the accumulated rotation established by LeBlanc *et al.* [2010] was modified for dense sand. The power dependency for a growing number of cycles reveals the maximum accumulated rotation for tests between one-way and two-way loading, as it was obtained for medium and loose sand. However, the magnitude of accumulated rotation increases for dense sand.
The logarithmic function for the change in soil stiffness obtained by LeBlanc *et al.* [2010] was also modified for piles embedded in dense sand. The increase of stiffness is found to be significantly bigger for dense sand comparing to medium and loose sand.
The results reveal that first cycles are important for a whole cyclic process, as the most of rotation is mobilized in these first cycles. This is undoubtedly influenced by the nonlinear increase of stiffness in its initial cyclic part. As the soil-pile system becomes more stiff, the accumulated rotation is more constant for larger number of cycles.

Furthermore, a series of post-cyclic tests revealed the increase of post-cyclic bearing capacity for both one-way and two-way cyclic loading. Following results contradicts current design standards, which involves degradation of stiffness for p-y curves by factor of 0.9 for including the effects of cyclic loading.

For more thorough summary of cyclic loading behavior of offshore monopiles in dense sand further research, focused on larger diversification of load characteristics, ought to be conducted. Finally, in order to create the general design method, obtained data must be compared with full scale results to verify proposed solutions.

References

API, American Petroleum Insitute. 2005. *Recommended practice for planning, designing and constructing fixed offshore platform*. Downloaded: 10-10-2013.

DNV, Det Norske Veritas. 2011. *Design of Offshore Wind Turbine Structures*. Downloaded: 10-10-2013.

EWEA, The European Wind Energy Association. 2013. *Wind in power - 2012 European Statistics*. URL: `http://www.ewea.org/`. Downloaded: 06-03-2014.

Ibsen, L. B., Hanson, M., Hjort, T., & Thaarup, M. 2009. MC- Parameter Calibration for Baskarp Sand No. *Department of Civil Engineering, University of Aalborg*.

LeBlanc, C., Houlsby, G.T., & Byrne, B.W. 2010. Response of stiff piles in sand to long-term cyclic lateral loading. *Geotechnique 60*, **No.2**, 79–90.

Lin, S., & Liao, J. 1999. Permanent Strains of Piles in Sand due to Cyclic Lateral Loads. *Journal of Geotechnical and Geoenvironmenral Engneering*, 798–802.

Little, Robert L., & Briaud, Jean-Louis. 1998. Full scale cyclic lateral load tests on six single piles in sand. *US Army Engineering District, Final Raport*.

Long, J.H., & Vanneste, G. 1994. Effects of Cyclilc Lateral Loads on Piles in Sand. *Journal of Geotechnical Engineering*, **Vol.120, No.1**, 225–244.

Onofrei, M.G., Roesen, H. Ravn, & Ibsen, L. Bo. 2012. Small-Scale Modelling of Monopiles in Sand Subjected to Long-Term Cyclic Load. *Department of Civil Engineering, Aalborg University*.

Sørensen, S.P.H., Brødbæk, K.T., Møller, M., & Augustesen, A.H. 2012. Review of laterally loaded monopiles employed as the foundation for offshore wind turbines. *DCE Technical Reports, Department of Civil Engineering, Aalborg University, Aalborg, Denmark*, **No.137**.

Recent publications in the DCE Technical Memorandum Series

DCE Technical Memorandum no. 45, Response of a stiff monopile for a long-term cyclic loading, Aleksandra Lada, Szymon Gres, Giulio Nicolai and Lars Bo Ibsen, June 2014.

DCE Technical Memorandum no. 46, The stiffness change and the increase in the ultimate capacity for a stiff pile resulting from a cyclic loading, Aleksandra Lada, Lars Bo Ibsen and Giulio Nicolai, June 2014.

DCE Technical Memorandum no. 47, The behaviour of the stiff monopile foundation subjected to the lateral loads, Aleksandra Lada, Lars Bo Ibsen and Giulio Nicolai, June 2014.

ISSN 1901-7278
DCE Technical Memorandum No. 45